Chapter 3

The Hodgkin-Huxley Model

§ 1.   The Neuron in Action I: Channel Gates

The 1952 papers by Hodgkin and Huxley on the physiology of the giant axon of the squid were a major milestone in the science of the nervous system. In the years that followed, one researcher after another were able to successfully model other axons and entire neurons based on the modeling schema first presented by Hodgkin and Huxley. The Hodgkin-Huxley model is here called a "modeling schema" rather than just a "model" because as more details have been learned regarding the physiology of the neuron, the basic H-H circuit model has been extended to include these details. The fact that the model *can be* so extended without fundamentally changing the general picture presented by Hodgkin and Huxley is why it is a "schema" rather than merely one single model.

The Hodgkin-Huxley model paper [HODG] was the fifth and culminating paper in a series of five published the same year [HODG1-4]. It introduces the model in Figure 2.3 of chapter 2 and goes on to derive from their experimental data the mathematical formulation of the model.

> Our experiments suggest that G_{Na} and G_K are functions of time and membrane potential, but that E_{Na}, E_K, V_{lk}, C, and G_{lk} may be taken as constant. The influence of the membrane potential on permeability can be summarized by stating: first, that depolarization causes a transient increase in sodium conductance and a slower but maintained increase in potassium conductance; secondly, that these changes are graded and that they can be reversed by repolarizing the membrane. In order to decide whether these effects are sufficient to account for complicated phenomena such as the action potential and refractory period, it is necessary to obtain expressions relating the sodium and potassium conductances to time and membrane potential. . . The first point which emerges is that the change in permeability appears to depend on membrane potential and not on membrane current. At a fixed depolarization the sodium current follows a time course whose form is independent of the current through the membrane. . . Further support for the view that membrane potential is the variable controlling permeability is provided by the observation that restoration of the normal membrane potential causes the sodium or potassium conductance to decline to a low value at any stage of the response [HODG][1].

The membrane at rest is said to be *polarized* because the resting potential is negative with respect to the outer tissue fluid of the extracellular region. Raising the membrane potential toward zero volts is called *depolarization*. Hodgkin and Huxley had discovered the existence of voltage-gated ion channels whose conductance was a function of V_m. They had further discovered that there were two distinct types of VGCs, today known as *transient channels* (Na^+) and *persistent channels* (K^+). These are illustrated in Figure 3.1.

---

[1] The symbols appearing in this quote have been altered to conform to the notation used in this book.
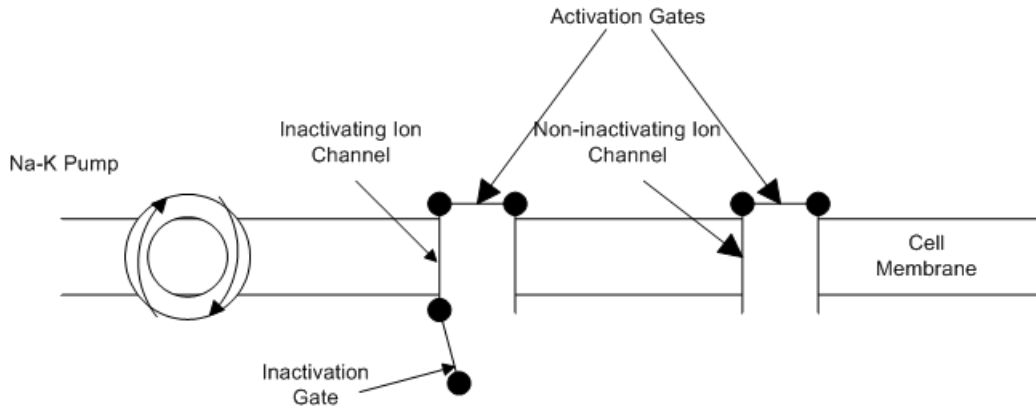
Figure 3.1: Qualitative model of transient ("inactivating") and persistent ("non-inactivating") ion channels in the cell membrane. Also depicted is the Na^+-K^+ pump.

This picture is not the same as the mechanism envisioned by Hodgkin and Huxley in 1952. At the time, the biophysical mechanism for transient and persistent channels was completely unknown and the data available did not implicate the membrane-spanning proteins as the site of ion conduction. Hodgkin and Huxley were able to rule out an earlier hypothesis they had made about the mechanism [HODG5]. Their 1952 data contradicted this earlier model and forced them to come up with another idea. Their new hypothesis turns out to be one which is retained (albeit in altered form) in the present day theory:

> A different form of hypothesis is to suppose that sodium movement depends on the distribution of charged particles which do not act as carriers in the usual sense, but which allow sodium to pass through the membrane when they occupy particular sites in the membrane. On this view the rate of movement of the activating particles determines the rate at which the sodium conductance approaches its maximum but has little effect on the magnitude of the conductance. It is therefore reasonable to find that the temperature has a large effect on the rate of rise of sodium conductance but a relatively small effect on its maximum value. In terms of this hypothesis one might explain the transient nature of the rise in sodium conductance by supposing that the activating particles undergo a chemical change after moving from the position which they occupy when the membrane potential is high. An alternative is to attribute the decline of sodium conductance to the relatively slow movement of another particle which blocks the flow of sodium ions when it reaches a certain position in the membrane.

> Much of what has been said about the changes in sodium permeability applies equally to the mechanism underlying the change in potassium permeability. In this case one might suppose that there is a completely separate system which differs from the sodium system in the following respects: (1) the activating molecules have an affinity for potassium but not for sodium; (2) they move more slowly; (3) they are not blocked or inactivated [HODG].

Today we know that "the distribution of charged particles which do not act as carriers . . . but which allow sodium to pass . . . when they occupy particular sites in the membrane" is accounted for by membrane-spanning proteins. The same is true for the putative "blocking particle" that was proposed to explain the transient nature of the sodium current, and likewise for the potassium current. The graded nature of the conductances led Hodgkin and Huxley to propose that there

were many independent sites where ion conduction could occur, and that these sites activated (and in the case of Na^+, inactivated) at different times according to a statistical law and in accord with the Boltzmann distribution of statistical mechanics. In 1952 this was all the farther Hodgkin and Huxley were willing to go insofar as speculation on a biophysical mechanism was concerned. Modern day *pore theory* of membrane-spanning proteins developed from later studies carried out in the 1960s and 1970s [ARMS1-6], [HILL1-3], [BEZA]. Pore theory gives us our current understanding of the physiological mechanism underlying the Hodgkin-Huxley dynamics.

According to the present theory, a channel pore conducts all-or-nothing according to whether its *ion gates* are open or closed. An open channel conducts with a single-pore conductance g_p. The total membrane conductance G is the sum of the conductances of all the open channels. A transient channel has two ion gates, the activation gate and the inactivation gate. Accordingly, this channel is seen as having three states: (1) deactivated (activation gate closed, inactivation gate open); (2) activated (both gates open); and (3) inactivated (inactivation gate closed). A persistent channel has only two states, activated and deactivated, because it has only one gate.

The statistical model of channel conductance holds that individual channel gates open or close independently of one another (but as a function of membrane voltage) in a probabilistic fashion. The mathematical theory of this is called *kinetics theory*. Hodgkin and Huxley assumed the gating function (which they described in terms of the above-mentioned "particles") followed the simplest possible process, namely a *first order rate process*. Let π_o denote the probability a gate is open. Let π_c denote the probability a gate is closed. Since these are the only two possibilities in a first order rate process, we have $\pi_o + \pi_c = 1$ or $\pi_c = 1 - \pi_o$. The *rate* at which closed gates transition to an open state is governed by a *rate constant*, α, which has units of 1/time and is a function of membrane voltage but not of time. The rate at which open gates transition to the closed state is governed by another rate constant, β. The probability of a gate being in the open state is then governed by the first-order *rate equation*

$$\frac{d\pi_o}{dt} = \alpha \cdot (1 - \pi_o) - \beta \cdot \pi_o. \tag{3.1}$$

The term multiplying α in (3.1) is the probability the gate is closed at time t. When the voltage on the membrane is held constant (3.1) is a linear differential equation and has for its solution

$$\pi_o(t) = \pi_o(0) \cdot \exp[-(\alpha + \beta)t] + \frac{\alpha}{\alpha + \beta} \cdot (1 - \exp[-(\alpha + \beta)t]), \quad t \geq 0 \tag{3.2}$$

where $\pi_o(0)$ is the initial condition. The quantity $\tau = (\alpha + \beta)^{-1}$ is called the time constant of the rate process at constant membrane potential. The dimensionless quantity $\alpha/(\alpha + \beta) = \tau\alpha$ is the steady-state probability at constant membrane potential. $\pi_o(t)$ is interpreted as the average fraction of the total available gates that are open at time t.

§ 2. The Neuron in Action II: The Channel Conductances

Hodgkin and Huxley were able to fit expressions for the rate constants for each of the three gates shown in Figure 3.1 and were able to use the resulting probabilities to describe the channel conductances for the sodium and potassium channels. In order to keep track of the three types of gates they gave their π_o values identifying symbols. They designated the potassium channel probability π_o by the letter n and identified its rate constants as α_n and β_n. τ_n and n_0 denote the time constant and the steady-state probability for the potassium gate, respectively. Letting V_r denote the resting potential of the membrane and defining $u = V_m - V_r$, where V_m is the membrane potential from chapter 2, they found that the rate constants for the potassium channel in the squid giant axon could be fit by the expressions

$$\begin{aligned} \alpha_n &= \frac{0.01\,(10 - u)}{\exp[1 - 0.1\,u] - 1} \\ \beta_n &= 0.125\,\exp[-u/80] \end{aligned} \qquad . \tag{3.3}$$

The constants in (3.3) are experimental values used to fit the model to their experimental data. The rate constants in these expressions have units of reciprocal milliseconds and u is expressed in millivolts relative to the resting potential. Later researchers studying different animal axons and different neuron cells learned that these constants depend on the type of neuron being studied. To this date no general theory has been produced that is capable of deriving the phenomenological constants from more fundamental principles.

The conductance of the potassium channel was empirically expressed as a power function of the open probability n. Letting g_K denote the maximum potassium channel conductance, Hodgkin and Huxley found they could express the K^+ channel conductance as

$$G_K = g_K \cdot n^4. \tag{3.4}$$

Investigators studying other types of cells have found that the fourth power expression for n does not hold universally, and have sometimes obtained n^3 relationships for voltage-gated potassium channels. Today it is known that there are many different species of potassium-conducting voltage-gated membrane proteins, and this fact is regarded as explaining why different exponents

for *n* have been observed in different types of cells.

Hodgkin and Huxley designated the open probability for the activation gate of the sodium channel by the symbol *m* and designated its rate constants by α_m and β_m. Their empirical expressions for these rate constants were

$$\alpha_m = \frac{0.1\,(25-u)}{\exp[2.5-0.1\,u]-1}$$
$$\beta_m = 4\,\exp[-u/18] \tag{3.5}$$

Here again, the rate constants are in units of reciprocal milliseconds and *u* is in millivolts. The transient sodium channel also has an inactivation gate. The expression for this gate is denoted by *h* with rate constants α_h and β_h. The empirical expressions for the rate constants were

$$\alpha_h = 0.07\,\exp[-u/20]$$
$$\beta_h = \frac{1}{\exp[3-0.1\,u]+1} \tag{3.6}$$

One can immediately note that the expressions for the rate constants for *h* differ in form from those of the two activation gates. The explanation for this is straightforward. Probability *h* is the open probability for the inactivation gate and therefore denotes *the probability that the sodium channel is **not inactivated***. By contrast, the other two expressions for the rate constants denote the probability that the channel *is **not deactivated***. For the potassium channel this is equivalent to saying the channel *is **activated***.

The sodium channel conductance is a function of both *m* and *h*. Letting g_{Na} denote the maximum sodium channel conductivity, Hodgkin and Huxley found the empirical expression for the sodium channel conductance to be

$$G_{Na} = g_{Na} \cdot m^3 h \ . \tag{3.7}$$

In the years that have passed since the publication of the Hodgkin-Huxley model, many researchers have found that expressions (3.4) and (3.7) have successfully described a great variety of different types of voltage-gate ion channels. Thus, one can generalize these equations for the many known cases of VGCs as

$$G_X = g_X \cdot m^p h^q \tag{3.8}$$

where *m* follows an expression similar to (3.3) or (3.4), *h* follows an expression similar to (3.6), *p*

is typically an integer greater than or equal to 1, and q is either 0 or 1. Where $q = 0$, the channel is a persistent (non-inactivating) channel (like the H-H potassium channel). Where $q = 1$, the channel is a transient (inactivating) channel. Thus it has turned out that the Hodgkin-Huxley model forms have constituted a model schema for a variety of voltage-gated ion channels.

The steady-state open probabilities for the three gates are denoted by n_∞, m_∞, and h_∞. It is instructive to plot these steady-state values as a function of relative membrane potential, u, as shown in Figure 3.2 below. A positive value for u means the membrane is depolarized. A negative value means the membrane is hyperpolarized. At the resting potential ($u = 0$ mV) few of the Na$^+$ activation gates, less than 10%, are activated. Approximately 70% of the Na$^+$ gates are not inactivated. In contrast, roughly 25% of the K$^+$ gates are activated. This means that the sodium conductance at rest is much smaller than the potassium conductance.

Depolarizing the membrane produces a rapid increase in the percentages of open Na$^+$ and K$^+$ activation gates, but it also produces a large drop in the number of open Na$^+$ inactivation gates. A depolarization of approximately 75 mV results in inactivation of virtually all the Na$^+$ channels in
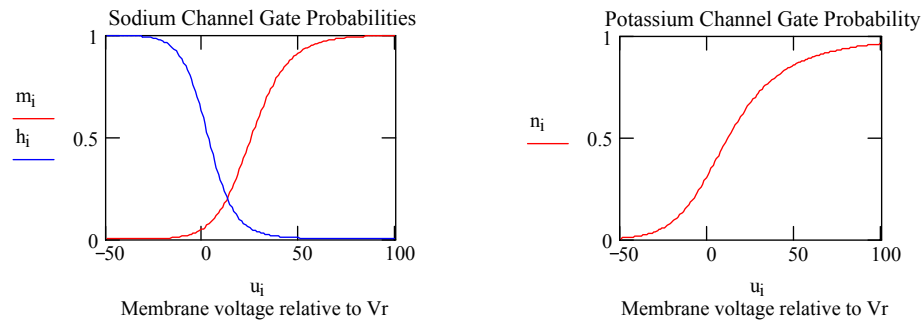
Figure 3.2: Steady-state gate probabilities vs. relative membrane voltage u for squid axon.
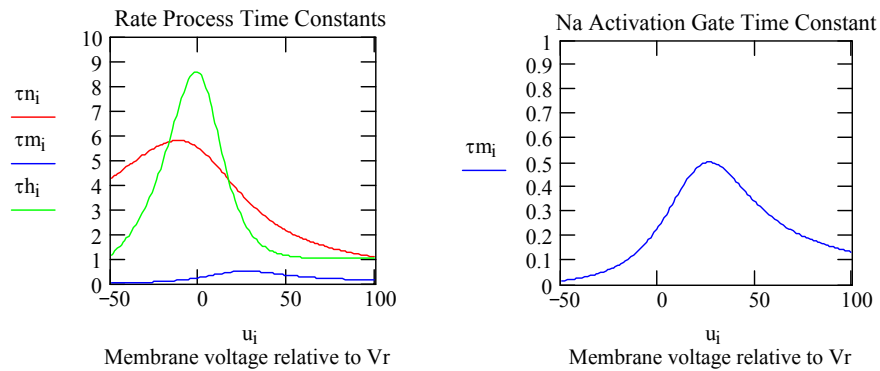
Figure 3.3: Rate process time constants for the K$^+$ activation gate and the Na$^+$ activation and inactivation gates. The graph on the right is a scale enlargement of the Na$^+$ activation gate time constant.

the steady state. Here, however, is where the rate process time constants τ_n, τ_m, and τ_h become important factors. Figure 3.3 shows the steady-state time constants for the three gates. At rest τ_m is much smaller than the other two time constants, approximately 0.2 ms compared to roughly 5.5 ms for τ_n and roughly 8.5 ms for τ_h. This means the Na$^+$ activation gate opens rapidly in response to depolarization compared to the other two gates. A depolarizing stimulus – for example, an inrush of Na$^+$ from ligand-gate ionotropic channels at a synapse – will rapidly open more voltage-gated Na$^+$ channels, which will increase the inward flow of Na$^+$ currents, which in turn will further depolarize the membrane. If a sufficiently large stimulus – on the order of a few mV – is initially applied, the process becomes regenerating and leads to the production of a large membrane depolarization, i.e., an action potential. The K$^+$ activation gate and the Na$^+$ inactivation gate lag behind this process by a few milliseconds before the former opens in large numbers and the latter close in large numbers, thereby repolarizing the membrane and bringing the action potential to an end. Here we may note that τ_h drops below τ_n for depolarization greater than about 15 mV. This means it is the closing of the Na$^+$ inactivation gates that is largely responsible for determining the peak value of the action potential because these gates now respond more quickly to the depolarization than do the K$^+$ activation gates.

§ 3.   The Dynamical System

Hodgkin and Huxley found maximum conductances per unit area of g_{Na} = 120 mS/cm^2, g_K = 36 mS/cm^2, and G_{lk} = 0.3 mS/cm^2, with G_{lk} found to be not dependent on membrane voltage. These values were deduced from their curve-fitting procedure to match the model to experiments. The membrane capacitance per unit area was found to be 1.0 µF/cm^2. Their reported battery potentials were expressed relative to the membrane resting potential V_r. That is, for ion X the reported battery potential was $V_X = E_X - V_r$. Their squid values were V_{Na} = 115 mV, V_K = –12 mV, and V_{lk0} = 10.613 mV. The value for V_{lk0} was chosen by forcing the total ionic current at the resting potential, i.e. $I_{Na} + I_K + I_{lk} = 0$ at $u = 0$. It is therefore purely a "curve fit" value. For a resting potential of V_r = –60 mV, these would correspond to E_{Na} = 55 mV, E_K = –72 mV, and a leakage potential of V_{lk} = –49.387 mV, respectively. Using these values in combination with the rate process variables in §2, they were able to numerically produce an action potential model that stood in very good agreement with experimentally measured action potentials.

The complete Hodgkin-Huxley model consists of the differential equation for the circuit of Figure 2.3 and the three differential equations describing the rate processes. Summarizing the four model equations, we get

$$C\frac{dV_m}{dt} = -G_{Na}\left(V_m - E_{Na}\right) - G_K\left(V_m - E_K\right) - G_{lk}\left(V_m - V_{lk}\right) \tag{3.9a}$$

$$\frac{dn}{dt} = -\left(\alpha_n + \beta_n\right)n + \alpha_n \tag{3.9b}$$

$$\frac{dm}{dt} = -\left(\alpha_m + \beta_m\right)m + \alpha_m \tag{3.9c}$$

$$\frac{dh}{dt} = -\left(\alpha_h + \beta_h\right)h + \alpha_h \tag{3.9d}$$

with the conductances G_X and the voltage-dependent rate constants as given previously. Using the parameter units of Hodgkin and Huxley, the ionic currents on the right-hand side of (3.9a) are in microamperes per square cm. The kinetic probabilities (3.9b-d) are dimensionless. The three channel time "constants" from (3.9a), C/G_X, come out in milliseconds.

Equations (3.9) are coupled through the dependence of the rate "constants" on V_m and the dependence of the conductances G_X on the probabilities n, m, and h. Thus the system represented by equations (3.9) is equivalent to a representation in terms of a fourth-order *nonlinear* ordinary differential equation. There is no known closed form solution for this equation, and so to compute the consequences of the model, numerical solution of system (3.9) is required. Hodgkin and Huxley described the algorithm they used for this in their 1952 paper. The need to introduce such an algorithm is what carries [HODG] beyond pure physiology research and into the arena of *computational* neuroscience.

Having no computer in 1952 on which to carry out this numerical solution, Hodgkin's and Huxley's numerical algorithm was one that was convenient for manual calculation using the tools available at the time. For this reason, we will not describe their algorithm here but will instead next examine a simple algorithm suitable for implementation on a modern computer. The method described here is called ***Euler's method***. Euler's method is not the most efficient algorithm known for carrying out the computational task; far more efficient numerical methods are available today [SMIT], [MILL]. But it is the easiest method to understand and, at this point in this text, this consideration is of higher importance. We consider a general first-order differential equation of the form

$$\frac{dy(t)}{dt} = f[y(t)] \; .$$

We integrate both sides of this equation with respect to time. For the left-hand side this gives us

$$\int_{t}^{t+\Delta t} \frac{\partial y(\tau)}{\partial \tau} d\tau = \int_{y(t)}^{y(t+\Delta t)} dy = y(t+\Delta t) - y(t) \ .$$

For the right-hand side, if Δt is small we can approximate the integral using the rectangle rule,

$$\int_{t}^{t+\Delta t} f[y(\tau)] d\tau \approx \Delta t \cdot f[y(t)] \ .$$

The error in making this approximation is a function of Δt and the slope of the function f. An analysis of error [CONT: 284-285] shows the approximation error to be

$$E = \frac{1}{2} \frac{df(t)}{dt} (\Delta t)^2 \ .$$

Thus, in computer analysis of the Hodgkin-Huxley equations one needs to be careful in selection of the discrete time step size. A sensible precaution is to try small variations in the selected value for Δt. If the percentage change in the computed result is less than the percentage change made in Δt, then the computation is *insensitive* to step size for this range of Δt. Otherwise the computation is *sensitive* to Δt and the interval should be reduced.

Applying this method to the gating probabilities in (3.9) and letting x denote any of n, m, or h, we have

$$x(t+\Delta t) = \left(1 - \frac{\Delta t}{\tau_x}\right) x(t) + \frac{\Delta t}{\tau_x} x_\infty \qquad (3.10a)$$

where

$$\tau_x = \frac{1}{\alpha_x + \beta_x}, \qquad x_\infty = \frac{\alpha_x}{\alpha_x + \beta_x} = \tau_x \alpha_x \qquad . \qquad (3.10b)$$

Here it is to be noted that the rate constants are functions of $V_m(t)$. From (3.10a) we see that the solution is given in terms of the ratio of Δt to the time constants τ_x . For good numerical accuracy one should select Δt to be much smaller than the smallest τ_x . From Figure 3.3, this would place Δt in the range of about 0.01 ms or less.

Applying Euler's method to the membrane voltage equation, we obtain

$$V_m(t+\Delta t) = \left(1 - \frac{\Delta t}{\tau_c}\right) V_m(t) + \frac{\Delta t}{\tau_{Na}} E_{Na} + \frac{\Delta t}{\tau_K} E_K + \frac{\Delta t}{\tau_{lk}} V_{lk} \qquad (3.11a)$$

where

$$\tau_c = \frac{C}{G_{Na} + G_K + G_{lk}} , \quad \tau_{Na} = \frac{C}{G_{Na}} , \quad \tau_K = \frac{C}{G_K} , \quad \tau_{lk} = \frac{C}{G_{lk}} . \qquad (3.11b)$$

Equations (3.10a) and (3.11a) are called ***difference equations***. Computer solution of the Hodgkin-Huxley equations calls for us to first convert the differential equations of (3.9) to the form of difference equations. The accuracy of the solution depends on how well these difference equations approximate their continuous-variable counterparts. Since a digital computer cannot actually solve differential equations – it can only solve difference equations – the technique used to obtain these difference equations is part of one's model representation in the system.

The widespread availability of programming languages capable of dealing with matrices and vectors makes it useful to re-express the difference equation calculation of the gate probabilities in vector-matrix form. The calculations called for by equation (3.10a) are expressed

$$\begin{bmatrix} n(t+\Delta t) \\ m(t+\Delta t) \\ h(t+\Delta t) \end{bmatrix} = \begin{bmatrix} (1-\Delta t/\tau_n) & 0 & 0 \\ 0 & (1-\Delta t/\tau_m) & 0 \\ 0 & 0 & (1-\Delta t/\tau_h) \end{bmatrix} \begin{bmatrix} n(t) \\ m(t) \\ h(t) \end{bmatrix} + \begin{bmatrix} (\Delta t/\tau_n)\, n_\infty \\ (\Delta t/\tau_m)\, m_\infty \\ (\Delta t/\tau_h)\, h_\infty \end{bmatrix} . \quad (3.12a)$$

By introducing matrix and vector notation we can write (3.12a) more compactly as

$$\mathbf{\Pi}(t+\Delta t) = \mathbf{A}_\pi \mathbf{\Pi}(t) + \mathbf{B}_\pi . \qquad (3.12b)$$

The terms in (3.12b) correspond in order to the vectors and the matrix in (3.12a).

§ 4.   The Dynamical System with Stimulus

In the absence of an external stimulus, the Hodgkin-Huxley dynamics just described settle into a steady-state at the resting potential $V_m = V_r$. In order to produce an action potential we must add to the basic model some sort of stimulus current, $I_s(t)$. This is depicted schematically in Figure 3.4. In the most general case current source I_s will itself be another model depicting the mechanism by which current is injected into the cytoplasm (positive numerical value of I_s) or is extracted from the cytoplasm (negative numerical value of I_s). The most common case found in the physiology literature uses an ideal current source that models the injection of a test current into the neuron. In this case $I_s(t)$ is merely some specified function (often a constant current turned on at some specified time t_{on} and turned off at some specified time t_{off}). For modeling a neuron *in vivo* I_s is often a model of an ionotropic synapse.
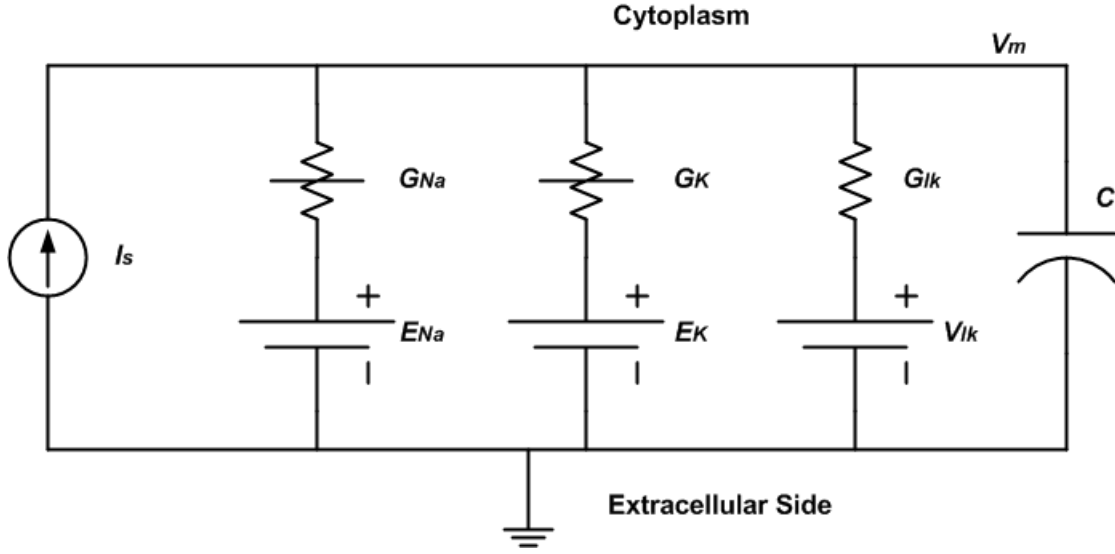
Figure 3.4: General Hodgkin-Huxley model with external stimulus.

The addition of current source I_s modifies equation (3.9a) by incorporating the I_s function. Applying Kirchhoff's current law to Figure 3.4 and re-arranging terms gives us

$$\frac{dV_m}{dt} = -\frac{1}{\tau_{Na}}\left(V_m - E_{Na}\right) - \frac{1}{\tau_K}\left(V_m - E_K\right) - \frac{1}{\tau_{lk}}\left(V_m - V_{lk}\right) + \frac{1}{C}I_s(t) \qquad (3.13)$$

where τ_{Na}, τ_K, and τ_{lk} are as defined in equation (3.11b). Converting this to a difference equation using Euler's method and expressing this result in vector notation gives us

$$V_m(t + \Delta t) = V_m(t) - \left[\frac{\Delta t}{\tau_{Na}} \quad \frac{\Delta t}{\tau_K} \quad \frac{\Delta t}{\tau_{lk}}\right]\begin{bmatrix} V_m(t) - E_{Na} \\ V_m(t) - E_K \\ V_m(t) - V_{lk} \end{bmatrix} + \frac{\Delta t}{C}I_s(t) . \qquad (3.14)$$

The addition of I_s does not alter equations (3.12).

The order in which calculations are performed is crucial for proper simulation of the Hodgkin-Huxley model. The following general algorithm illustrates the proper computation using Euler's method.

Algorithm 3.1: Hodgkin-Huxley Simulation Using Euler's Method

1. Initialize all parameters and initial conditions for the dynamical variables.
2. for $t = 0$ to $t = t_{final}$ in steps of Δt do the following steps
3.   compute $I_s(t)$ {the details of this step depend on the model for I_s}
4.   compute the six rate constants according to equations (3.3), (3.5), and (3.6) using $V_m(t)$

5. compute the three τ_x and x_∞ values according to equation (3.10b)
6. compute the three gate probabilities according to equation (3.12)
7. compute the new values for G_{Na} and G_K according to equations (3.7) and (3.4)
8. compute new values for τ_{Na} and τ_K according to equations (3.11b)
9. compute $V_m(t + \Delta t)$ according to equation (3.14); if $t < t_{final}$ increment t and repeat 3-9
10. Display and save desired results from the simulation; end simulation.

Figures 3.5 illustrate the generation of an action potential and the time course of the sodium and potassium conductances using Hodgkin's and Huxley's squid parameters. The resting values for G_{Na} and G_K are 0.0106 mS/cm^2 and 0.3666 mS/cm^2, respectively. The stimulus was a brief pulse of injected current with a current density of 2.5 μA/cm^2 applied at $t = 10$ ms and lasting for 5 ms. The Δt used in the simulation was 0.01 ms.

The effect of the stimulus on the membrane potential is clearly visible in the membrane voltage plot (note the change in V_m at $t = 10$ ms in Figure 3.5). The stimulus had sufficient amplitude and duration to trigger a self-generating rise in sodium channel conductance due to the positive feedback mechanism of voltage-gated sodium inrush current. This is clearly visible in the plot of G_{Na} vs. t at $t = 15$ ms. The steep rising edge of $G_{Na}(t)$ is called the ***depolarizing phase*** of the action potential dynamics. The peak of the action potential corresponds to the peak in G_{Na}. At this point (approximately 16 ms into the simulation) the effect of the sodium inactivation gate begins to be manifested in the sodium channel response. The Na$^+$ channel becoming inactivated, the buildup of V_m is brought to a halt. Concurrently, the rise of the potassium conductance G_K and its associated outflow of K$^+$ ions begins the process of ***repolarizing*** the cell. As the Na$^+$ channels inactivate, the K$^+$ current brings V_m back to the resting level and even causes it to undershoot this
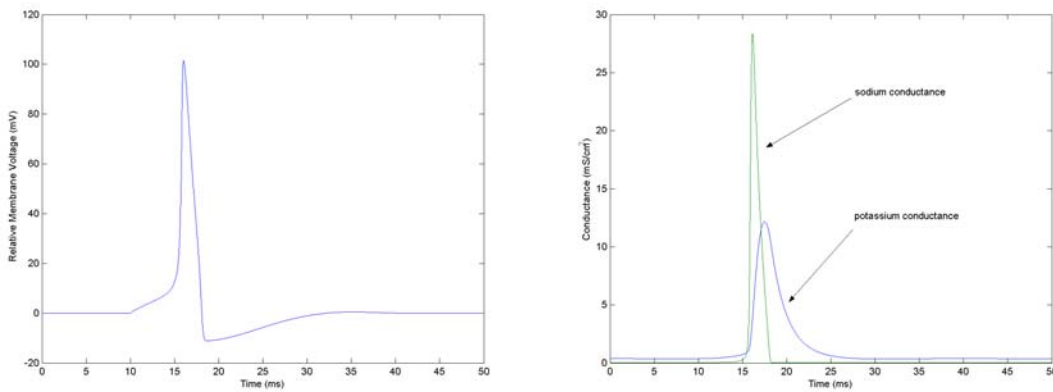
Figure 3.5: Membrane voltage (relative to resting potential) and voltage-dependent conductances for the Hodgkin-Huxley model of the squid.

level. This undershoot is called ***hyperpolarization*** of the membrane potential.

A smaller-amplitude stimulus or one of shorter duration would have produced a response in the membrane potential, but the change in V_m would not have been sufficient to induce self-generating activation of the sodium gates. Without this self-generating action, no action potential (AP) would result. This is called a ***threshold effect***, and the critical value of V_m associated with the effect is called the ***threshold***. However, the threshold is not a constant but, rather, depends on past activity. We can understand this from the following consideration.

The slower K^+ time constant, relative to the Na^+ channel, is clearly evident from the time courses of the two conductances. Although $h(t)$ for the inactivation gate is not shown in Figure 3.5, inspection of Figure 3.3 tells us the time constant for h is going to be even slower than that of the potassium activation gate variable n during the repolarizing phase. This means that the deactivation of the h gate proceeds more slowly than the recovery (deactivation) of the n gate. During this time when a large fraction of the sodium inactivation gates are closed, an additional stimulus cannot succeed in evoking more Na^+ current inrush into the cell. As more time passes and more h gates open, it becomes possible to re-stimulate another action potential, but the threshold required for doing so is increased above the normal resting level. This phenomenon is called the ***refractory period*** of the cell. It is divisible into two phases. The period during which no AP can be re-stimulated is called the ***absolute refractory period***. The phase during which it is possible to re-stimulate an AP (but at a higher threshold level) is called the ***relative refractory period***. During the relative refractory period, the threshold value for membrane potential undergoes an approximately exponential decay as a function of time, the time constant of this decay being a function of the time constants of both the h and n gates.[2]

The absolute value of V_r for the squid presents an interesting consideration. Hodgkin's and Huxley's squid parameters do not allow us to compute the absolute (relative to the extracellular region) numerical value of the resting potential. Later models of neurons often provide this information as part of their phenomenological expressions. But for Hodgkin's and Huxley's squid, we must have additional information if we are to estimate the actual resting potential of the cell membrane. For this we can turn to another Nobel laureate, Bernard Katz. Katz tells us the ion concentrations for the squid axon are $[Na^+]_o = 460$ mM, $[Na^+]_i = 50$ mM, $[K^+]_o = 10$ mM, and $[K^+]_i = 400$ mM [KATZ]. Plugging these values into the Nernst potential equation from chapter 2,

---

[2] In a simulation one can, of course, apply as arbitrarily large a stimulus as one desires. The simulation will dutifully show the effect of such a stimulus on V_m. However, a degree of common sense is required here. One thing not represented in the Hodgkin-Huxley model is the effect such a large stimulus current will have on the living cell. To put it bluntly, "the model does not know" that the living cell can be electrocuted. If the modeler also does not realize this, some ridiculous conclusions might be drawn. This is another example of why we say a *system* is both the object *and* its representation (the model).

we get

$$\frac{E_{Na}}{E_K} = \frac{\ln(460/50)}{\ln(10/400)} = -0.60 \ .$$

To be consistent with the relative Hodgkin-Huxley battery potentials, we must have

$$\frac{115 + V_r}{-12 + V_r} = -0.60$$

from which we obtain an estimate of $V_r = -67.4$ mV. This value is close to the ballpark figure of –65 mV many biology textbooks use as their typical example value of membrane potential. However, there is an interesting problem that crops up with using the Katz values in conjunction with the Hodgkin-Huxley battery parameters. We will explore this in one of the exercises at the end of this chapter.

In an earlier paper published in 1949 [HODG6], Hodgkin and Katz reported an experimental value of –47.5 mV for the resting potential of the squid axon. However, they commented, "The true values of the membrane potential are likely to be 5 – 15 mV higher than those recorded experimentally" because of certain sources of measurement error in the test method. Many present day biology textbooks are happy to take them at their word for this and use a "standard" V_r of –60 mV for the squid axon. This would place E_{Na} at an absolute value of 115 – 60 = 55 mV assuming Katz's [Na$^+$] numbers above at a temperature of 15 °C (the temperature at which the 1949 data was taken). However, it is easily shown that this temperature used with the [K$^+$] values given above predicts $E_K = -91.4$ mV, which is inconsistent with both V_r and the Hodgkin-Huxley parameter for the potassium battery. A more "up to date" value for K$^+$ concentrations in squid is given by Koester and Siegelbaum as [K$^+$]$_o$ = 20 mM, [K$^+$]$_i$ = 440 mM [KOES]. This gives us $E_K =$ –74.2 mV at this temperature and implicates a H-H potassium battery parameter of –14.2 mV (rather than –12 mV)[3]. We can see from all this that model reconciliation with a broader context of facts can be an interesting exercise, and that even the most successful models do not always show an immediate fit to "other facts." Indeed, even in [HODG] Hodgkin and Huxley noted certain problems with getting their model to agree with the equation for the Nernst potential. They commented,

> The results presented here show that the equations derived in Part II of this paper predict with fair accuracy many of the electrical properties of the squid giant axon: the form, duration and amplitude of

---

[3] Actually, there is even less discrepancy because the temperature for the data used in deriving the parameters in [HODG] was only 6 to 7 °C, and this places both battery potentials in the H-H model well within the experimental accuracy of the measuring equipment they used.

spike, both 'membrane' and propagated; the conduction velocity; the impedance changes during the spike; the refractory period; ionic exchanges; subthreshold responses; and oscillations. . . This is a satisfactory degree of agreement, since the equations and constants were derived entirely from 'voltage clamp' records, without any adjustment to make them fit the phenomena to which they were subsequently applied. . .

The agreement must not be taken as evidence that our equations are anything more than an empirical description of the time-course of the changes in permeability to sodium and potassium. An equally satisfactory description of the voltage clamp data could no doubt have been achieved with equations of a very different form, which would probably have been equally successful in predicting the electrical behavior of the membrane. It was pointed out in Part II of this paper that certain features of our equations were capable of a physical interpretation, but the success of the equations is no evidence in favor of the mechanism of permeability change that we tentatively had in mind when formulating them.

The point that we do consider to be established is that fairly simple permeability changes in response to alterations in membrane potential, of the kind deduced from the voltage clamp results, are a sufficient explanation of the wide range of phenomena that have been fitted by solutions of the equations [HODG].

This is a good example of how Nobel laureates become Nobel laureates.

§ 5.   Repetitive Firing

If a constant stimulus test current is injected into many types of neurons, some form of repetitive firing pattern often develops. For the H-H model, the parameters of which model an axon, a steady frequency of repetitive firing is produced. This is shown in Figure 3.6. Below some threshold of stimulation a repetitive pattern is not produced. Rather, either no AP or one or two APs result. But above the threshold (approximately 6.5 μA/cm^2 for the H-H parameters), the cell fires with increasing frequency as the stimulus current I_s is increased. Furthermore, the onset of firing jumps from no repetitive firing to a relatively high rate abruptly for a small increase in I_s.
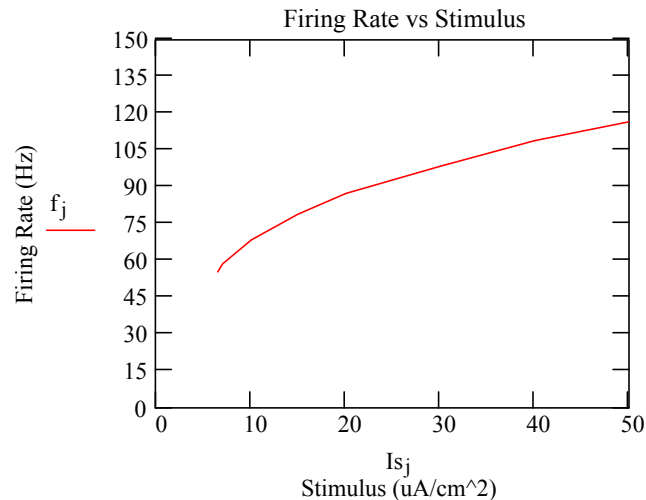

Figure 3.6: Firing rate of the H-H model vs. constant stimulus current

Of course, in a whole neuron the firing rate vs. stimulus tends to be set much more by the neuron's cell body and dendrites rather than by its axon. The function of the axon, after all, is to transmit APs rather than generate them. From this point of view it does not seem odd that the axon of a cell would have a more "hair-trigger" firing response than does the cell body.

A firing rate curve like Figure 3.6 where we find a discontinuity in the curve is called a ***type II model*** in the theoretical literature. There are some species of neurons where this discontinuity is not observed. Rather, the onset of firing rates rises from zero without a large jump from no-firing to high frequency firing. Neurons of this type are called ***type I model*** neurons. This variety in responses to test stimuli is caused by the existence of a great variety of voltage-gated channel proteins, a topic we will discuss later. The axon typically has only the Na^+ and K^+ channels described by the Hodgkin-Huxley model. However, in addition to the inactivating Na^+ channel of the original H-H model, it is now known that persistent (non-inactivating) Na^+-conducting proteins also exist, as do transient (inactivating) K^+ channels. Completing the picture, neurons also express voltage-gated Ca^{2+} channels of various types. The constant-stimulus-current test method is a key tool used by physiologists in studying different kinds of neurons and modeling them by extensions of the basic Hodgkin-Huxley schema. The great variety of VGCs expressed in nature leads to a great variety of different kinds of repetitive firing patterns, including those of some neurons that spontaneously fire, either repetitively or in bursts with long interludes in between (so-called "pacemaker" neurons). Most theoretical neuron models are parameterized to fit the firing patterns seen in response to the constant-current test stimulus.

Below the threshold for the on-set of repetitive firing, the membrane response exhibits an increase in the firing threshold. This is illustrated in Figure 3.7. We can note the decaying ringing following the second AP in the voltage response. The increase in threshold is caused by residual K^+ conductance, which the input stimulus causes to increase due to the increase in V_m this current
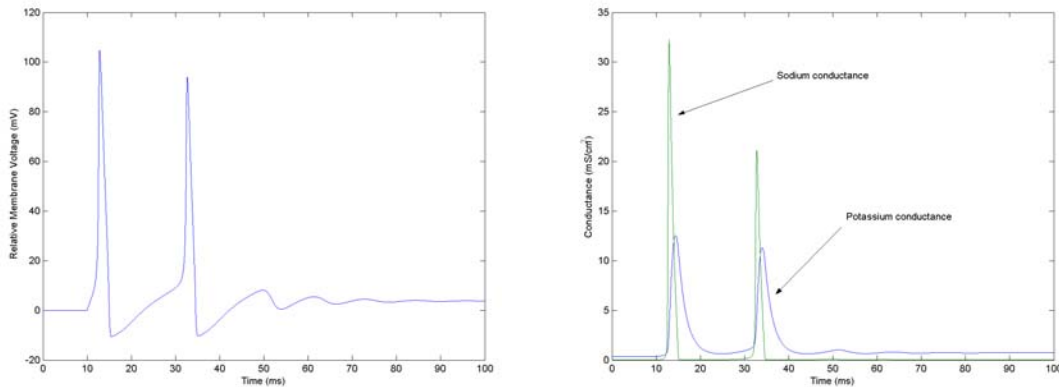
**Figure 3.7:** Constant-stimulus response for I_s = 6.0 μA/cm^2 for H-H squid model.

produces from the charges it injects into the cell. We can also note the dramatic decrease in the peak Na$^+$ conductance observed during the second AP. This is caused by the fact that the inactivation gates have not had time to return to equilibrium plus the fact that the stimulus current causes more inactivation gates to close through the mechanism of the small rise in V_m the stimulus produces (refer to the steady-state h curve in Figure 3.2). For $I_s = 6$ μA/cm^2 the squid axon model produces two APs spaced about 20 ms apart, by which we can tell that its minimum repetitive firing rate will be greater than 50 Hz (which ranks as a "high" firing rate in biological signal processing; some neurons are rarely capable or flatly incapable of firing at this fast).

§ 6.   Synaptic Signals

With the exception of sensory neurons and those neurons that received graded inputs via gap junction synapses, the majority of neurons in the central nervous system receive their inputs from chemical synapses in pulsed form. The synapse is in itself a very interesting system-within-the-system in models of biological signal processing. We will be discussing more details of the synapse model later in this text. But at this point it is appropriate to discuss empirical modeling of the signal seen by the postsynaptic cell in response to an AP from one of its sourcing presynaptic neurons. Specifically, we discuss those synaptic receptors that constitute ionotropic channels responding to ligand neurotransmitters (LGCs).

An ionotropic channel is added to the basic voltage-gated Hodgkin-Huxley-like compartment model as shown in Figure 3.8. The synapse is represented by a ligand-gated conductance G_{syn} and a synaptic potential E_{syn} that plays the same modeling role as the other batteries in the model. The
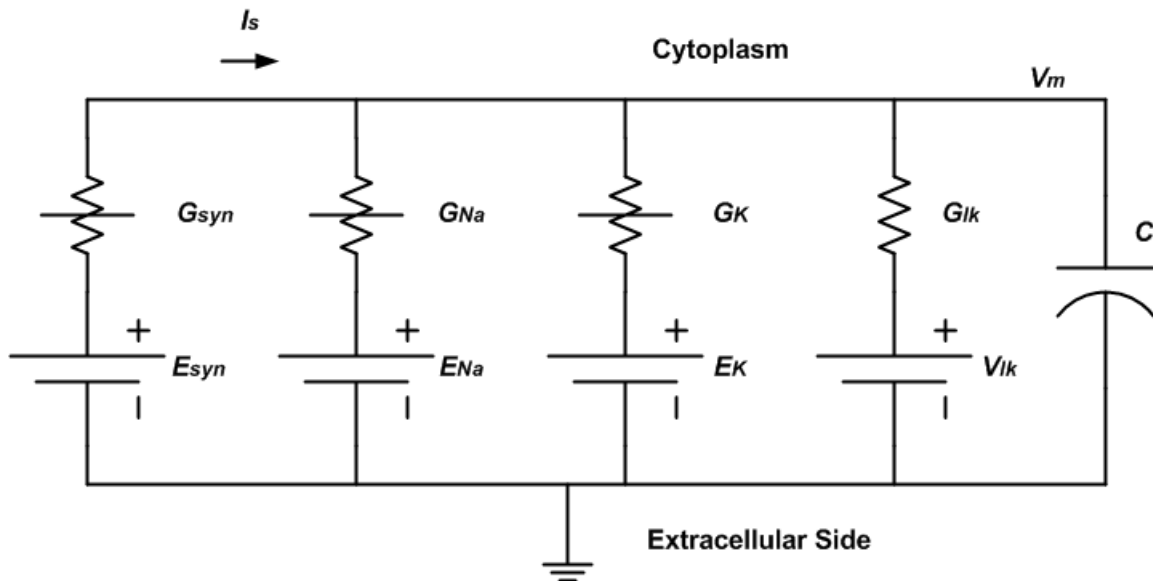
Figure 3.8: Hodgkin-Huxley compartment augmented by an ionotropic synapse channel.

ionotropic channels are broadly divisible into excitatory synapses (those where I_s is positive for the direction shown in Figure 3.8) and inhibitory synapses (those where I_s is negative for the direction shown). Whether the synapse is excitatory or inhibitory is incorporated into the model by the numerical value assigned to E_{syn}. If $E_{syn} > V_r$ then the synapse is excitatory. If $E_{syn} < V_r$ then the synapse is inhibitory. A typical value for an excitatory channel is $E_{syn} = 0$ mV. A typical value for an inhibitory channel is $E_{syn} = -70$ mV to -75 mV. Note that these are absolute values with respect to the extracellular fluid. If, as in Hodgkin's and Huxley's original model, the battery potentials for E_{Na}, etc. are normalized to V_r, then this same scaling must be applied to E_{syn}.

G_{syn} models the time-dependent response of the channel to the release of neurotransmitter from the presynaptic terminal of the source neuron. In general form, we may write $G_{syn} = g_{max} \cdot g(t)$ where g_{max} is the maximum conductance of the channel and $g(t)$ describes the time course of the channel conductance. By convention the maximum value of $g(t)$ is unity. In the absence of action potential stimulation of the presynaptic terminal, the steady-state value for $g(t)$ is zero. Empirical characterizations of synaptic conductance usually result in one or the other of two functions for $g(t)$, which we will denote as the **alpha function**, $g^{(\alpha)}(t)$, and the **beta function**, $g^{(\beta)}(t)$.

If the neurotransmitter release from the presynaptic terminal occurs at $t = 0$, the alpha function is described by the equation

$$g^{(\alpha)}(t) = \exp(1) \cdot \frac{t}{\tau} \cdot \exp[-t/\tau] \qquad (3.15)$$

where the exp(1) term is merely a scaling factor to make $g^{(\alpha)}(t)$ have a maximum value of one. The peak value of $g^{(\alpha)}(t)$ occurs at $t = \tau$ and $g^{(\alpha)}(t) = 0$ for $t < 0$.

Equation (3.15) describes the channel response to a single presynaptic action potential event. In order to obtain a more generally applicable model we must treat the alpha function in a somewhat more general way capable of incorporating multiple action potential events occurring at different moments in time. Preferably what we would like is a differential equation description for $g^{(\alpha)}(t)$ so that we can incorporate the calculation of $g^{(\alpha)}(t)$ into the rest of the simulation computation. The standard technique for accomplishing this in system theory is called the **state variable representation**. Let $V_{pre}(t)$ denote the membrane potential of the presynaptic cell, as measured at its presynaptic terminal, at time t. We define two quantities, $x_1(t)$ and $x_2(t)$, called the **state variables** of the channel. These are defined in such a way that we can write $g^{(\alpha)}(t)$ in terms of them using the vector-matrix notation of linear algebra,

$$g^{(\alpha)}(t) = \begin{bmatrix} 0 & \exp(1)/\tau \end{bmatrix} \begin{bmatrix} x_1(t) \\ x_2(t) \end{bmatrix} . \qquad (3.16)$$

In state-variable terminology, equation (3.16) is called an ***output equation***.

The two state variables are purely mathematical quantities for modeling the kinetics of the ionotropic channel. In this, their role is similar to that of the rate constants in the H-H voltage-gated channel models. They are described by a pair of differential equations, called the ***state equation***, which, in matrix form, is given as

$$\begin{bmatrix} dx_1(t)/dt \\ dx_2(t)/dt \end{bmatrix} = \begin{bmatrix} -1/\tau & 0 \\ 1 & -1/\tau \end{bmatrix} \begin{bmatrix} x_1(t) \\ x_2(t) \end{bmatrix} + \begin{bmatrix} 1 \\ 0 \end{bmatrix} \eta [V_{pre}(t)] . \qquad (3.17)$$

Here $\eta(t) = \eta[V_{pre}(t)]$ is an input function that describes the stimulation of the postsynaptic cell as a function of the presynaptic membrane potential. Physiologically, this function describes the action of neurotransmitter (NTX) release in the synapse. It is a ***thresholding function*** in that $V_{pre}(t)$ must exceed some threshold value Ω before the source cell will release its neurotransmitter. Biologically realistic values for Ω typically lie in the range of –20 to –30 mV. It is also an ***impulsive function*** in that neurotransmitter exocytosis tends to occur as a brief burst of NTX release that starts and ends over a very brief interval of time (well under 1 ms).

We obtain the difference equations required for simulation in the same manner as before by integrating both sides of equation (3.17). Here the only special consideration comes with integrating the input function $\eta(t)$ over the interval from t to $t + \Delta t$. Because of its impulsive nature, it is convenient to introduce a special function, H(z), known as ***Heaviside's unit step function***, named after the interesting and somewhat eccentric 19th-20th century British engineer Oliver Heaviside[4]. H(z) = 1 for argument $z > 0$ and H(z) = 0 for $z < 0$. As a practical matter, we will make H(0) = 0. Using this function, we may make the reasonable approximation

$$\int_t^{t+\Delta t} \eta(\tau)d\tau \approx v \cdot H[V_{pre}(t) - \Omega]$$

where v is a parameter characterizing the amount of neurotransmitter released by the presynaptic neuron. We will typically use $v = 1$, but other values can be used to model a number of short-term

---

[4] Heaviside (1850-1925) was one of the few members of the Royal Society to have his papers regularly turned down for publication. He was the despair of the mathematicians of his day because of his non-rigorous use of special functions in his "operational calculus." His proposed names for electrical units – pere, mac, tom, bob, and dick – somehow never caught on. He developed the theory of cable loading, which made the transatlantic cable possible, wrote Maxwell's equations in the form used today, pioneered the use of "phasors" (which every electrical engineering student comes to know well), and was the first to propose that an electrical charge would increase in mass as its velocity increases (which anticipated Einstein's later discovery). Heaviside was known for a sometimes caustic interpersonal style, which made him many enemies. When criticized by mathematicians for his vague meanings and definitions in his "operational calculus," he merely retorted, "Shall I refuse my dinner because I do not fully understand the process of digestion?"

modulation effects that occur in biological signaling. With this approximation we obtain the dynamical difference equations for $g^{(\alpha)}(t)$ as

$$\begin{bmatrix} x_1(t+\Delta t) \\ x_2(t+\Delta t) \end{bmatrix} = \begin{bmatrix} 1-\Delta t/\tau & 0 \\ \Delta t & 1-\Delta t/\tau \end{bmatrix} \begin{bmatrix} x_1(t) \\ x_2(t) \end{bmatrix} + \begin{bmatrix} v \\ 0 \end{bmatrix} H[V_{pre}(t) - \Omega] \qquad (3.18)$$

$$g^{(\alpha)}(t) = \begin{bmatrix} 0 & \exp(1)/\tau \end{bmatrix} \begin{bmatrix} x_1(t) \\ x_2(t) \end{bmatrix}. \qquad (3.19)$$

The beta function is defined as

$$g^{(\beta)}(t) = \gamma[\exp(-t/\tau_2) - \exp(-t/\tau_1)], \, t \geq 0 \qquad (3.20)$$

with $g^{(\beta)}(t) = 0$ for $t < 0$. γ is a normalizing factor making the peak value equal to one. For the time constants we have $\tau_1 < \tau_2$. The maximum value of the function occurs at $t = T_{pk}$ where

$$T_{pk} = \frac{\tau_1 \tau_2}{\tau_2 - \tau_1} \ln(\tau_2/\tau_1) \qquad (3.21)$$

and so

$$\gamma = \frac{1}{\exp(-T_{pk}/\tau_2) - \exp(-T_{pk}/\tau_1)}. \qquad (3.22)$$

The state variable equations for $g^{(\beta)}(t)$ are

$$\begin{bmatrix} dx_1(t)/dt \\ dx_2(t)/dt \end{bmatrix} = \begin{bmatrix} -1/\tau_1 & 0 \\ 0 & -1/\tau_2 \end{bmatrix} \begin{bmatrix} x_1(t) \\ x_2(t) \end{bmatrix} + \begin{bmatrix} 1 \\ 1 \end{bmatrix} \eta[V_{pre}(t)] \qquad (3.23)$$

$$g^{(\beta)}(t) = \begin{bmatrix} -\gamma & \gamma \end{bmatrix} \begin{bmatrix} x_1(t) \\ x_2(t) \end{bmatrix}. \qquad (3.24)$$

Integrating both sides of (3.23) to obtain the difference equations gives us

$$\begin{bmatrix} x_1(t+\Delta t) \\ x_2(t+\Delta t) \end{bmatrix} = \begin{bmatrix} 1-\Delta t/\tau_1 & 0 \\ 0 & 1-\Delta t/\tau_2 \end{bmatrix} \begin{bmatrix} x_1(t) \\ x_2(t) \end{bmatrix} + \begin{bmatrix} v \\ v \end{bmatrix} H[V_{pre}(t) - \Omega] \qquad (3.25)$$

with the output equation still given by (3.24).

Figure 3.9 illustrates the comparison of $g^{(\alpha)}(t)$ and $g^{(\beta)}(t)$ scaled to equivalent times for the peak response. We may note that generally, for equal peaking times, $g^{(\beta)}(t)$ has a slower decay and a slightly faster rising edge in its response compared to $g^{(\alpha)}(t)$. Therefore, the response of the Hodgkin-Huxley compartment to these two functions will be different.
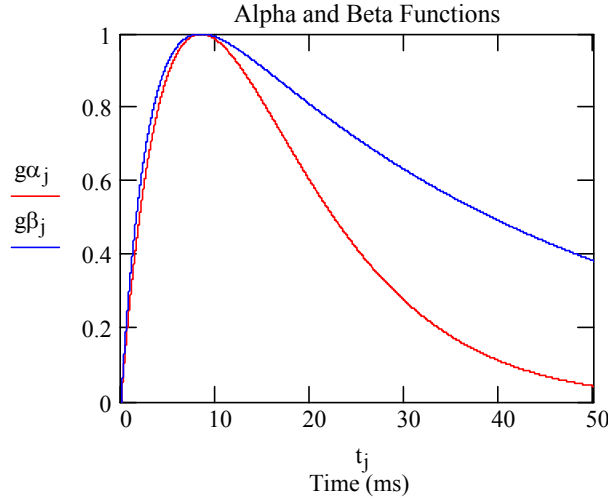
Figure 3.9: Comparison of the alpha- and beta- functions scaled to equivalent peak times

One of the major challenges in modeling ligand-gated channels (LGCs) is the determination of the maximum conductance parameter g_{max}. This parameter must depend on the single-channel conductance of an individual channel pore, g_p, and also on the number of such membrane-spanning channel pores present in the synapse. It must also depend on the *availability* of these proteins to bind with the neurotransmitter ligand, which is something that might depend on factors going on metabotropically within the cell such as phosphorylation/dephosphorylation activity. The empirical $G_{syn}(t) = g_{max} g(t)$ expression describes the average *synaptic* conductance resulting from the parallel combination of individual *pore* conductances.

Not surprisingly, experimental data for g_{max} is, to say the least, challenging to come by. We are dealing here with tiny amounts of current (on the order of about 2 pA per pore) in tiny patches of membrane. Furthermore, the g_p in which we are interested reside in synapses, which makes them very difficult to access with test and measuring equipment. Most of the experimental data reported in the literature is taken from channels outside synapses ("extra-synaptic" channels), and there is reason to suspect that receptors located outside the synapse may differ from those in synapses [SILV: 120].

The data we do have tells us that g_p values for the most part range from 10 pS to 50 pS across a wide variety of receptor types (both VGCs and LGCs), although there are also some in the 3 pS to 10 pS range [HILL4: 401]. The amount of surface area in a typical synapse is on the order of about 0.1 μm^2 (as a geometric-mean reference value; there is a great deal of variance in this parameter) [FIAL: 21]. At a reference density on the order of 100 channel proteins/μm^2 [HILL4: 377-404], this would place the number of channel pores in a typical synapse at about 10 single-channels per synapse, and a reference value of 20 pS/pore would place the value of g_{max} on the

order of about 200 pS per synapse. This value is more or less in agreement with experimental values reported in the literature [SEGE], but it should be viewed as a "ballpark figure" only and not at all as a precise determination. (Indeed, whether or not the phrase "typical synapse" has any real meaning – and if so, what? – can be debated). What we do know with confidence is that we can expect the numerical value of g_{max} to vary over a wide range, and that it is probably not really a constant even for one specific synapse (due to various physical-chemical processes that can modulate its value). For example, Gabbiani et al. reported g_{max} values of 720 pS and 1200 pS for two types of ionotropic synapses found in cerebellar granule cells [GABB]. (The two channels are known as AMPA and NMDA[5] channels, respectively). Segev and London cite ranges from 100 to 300 pS (AMPA) and 50 to 500 pS (NMDA) for synapses in neocortical neurons [SEGE].

As for the time constants in $G_{syn}(t)$, these are easier to determine experimentally. Different types of LGCs show different values for these time constants, and we will discuss them when we discuss specific LGCs. Here let it be enough to say they vary over a range from a few ms to several tens of ms. The values τ_1 = 3 ms and τ_2 = 40 ms used in Figure 3.9 were the values Gabbiani et al. found for the NMDA channel in the cerebellar granule cell. For the AMPA channel their reported time constants were τ_1 = 0.09 ms and τ_2 = 1.5 ms.

Finally, it is worth noting that more physiological models that take into account factors such as the concentration of neurotransmitter in the synaptic cleft have also been developed. These ***kinetics models*** describe the synaptic channel conductance using an approach similar to that used by Hodgkin and Huxley for the gating probabilities of the voltage-gated channels [MAGL1-2].

§ 7.   The Subthreshold Response

As noted earlier, action potential generation is a thresholding phenomenon. If the stimulus is insufficient to produce an action potential, the cell's response is called a ***subthreshold response***. Figure 3.10 illustrates the response of Hodgkin's and Huxley's squid axon model to a stimulus pulse of 2.5 μA/cm^2 applied at t = 10 ms for a duration of 2.5 ms. This is a subthreshold stimulation, and we can see that V_m rises less than 5 mV (relative to the resting potential) before the opening of the K$^+$ channels acts to repolarize V_m.

In chapter 1 it was said that the "leaky integrator" model is a popular phenomenological model for neuron responses. Figure 3.11 illustrates the response of the squid axon model excited by two

---

[5] AMPA stands for α-amino-3-hydroxy-5-methyl-4-isoxazole-proprionic acid. NMDA stands for N-methyl-D-aspartic acid. These are pharmacological compounds used to identify synaptic receptors. Both receptors respond to the neurotransmitter glutamate, and both are widely found in the central nervous system. Note, however, that AMPA and NMDA are names for species of synaptic receptors and within these classifications there are numerous different values for g_{max} found for different neurons.
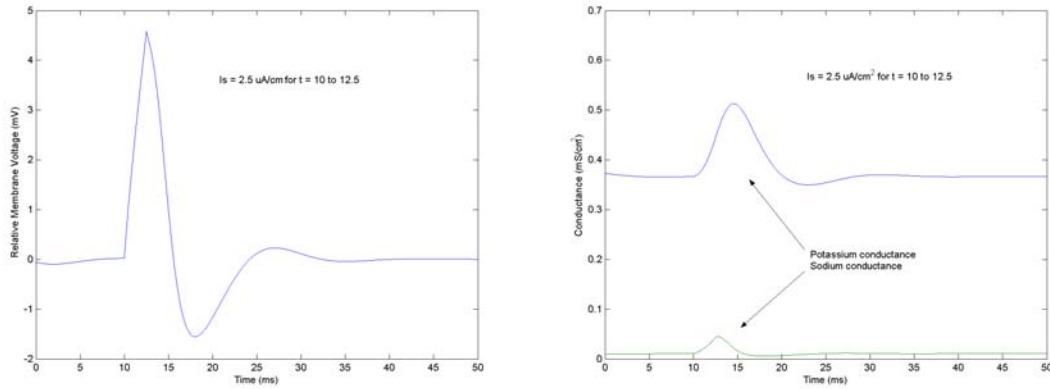
Figure 3.10: Subthreshold stimulation of the H-H squid axon model. The stimulus I_s from figure 3.4 was 2.5 μA/cm^2 with a duration of 2.5 ms.
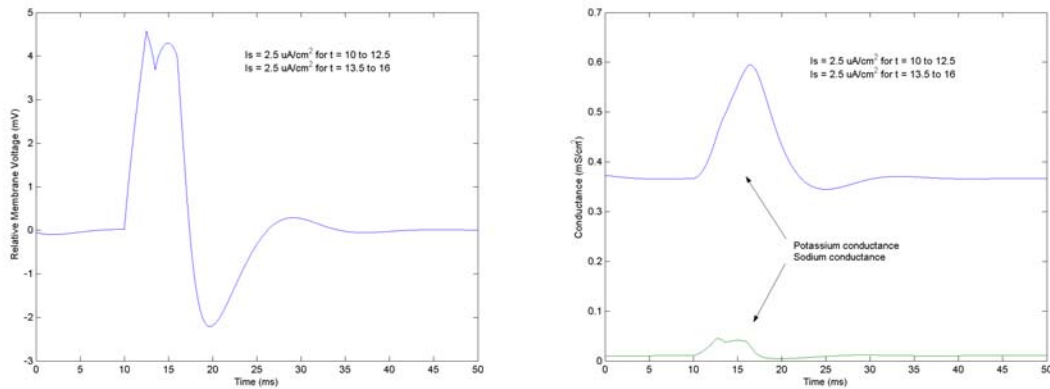
Figure 3.11: Subthreshold dipulse stimulation. The first pulse is the same as for figure 3.10. The second pulse is also 2.5 μA/cm^2 with a duration of 2.5 ms and is applied at t = 13.5 ms (1 ms after the end of the first pulse). We can observe a nonlinear "leaky integrator" action in this response. However, this "integrator" action is swiftly overcome by the onset of K$^+$ conductance.

stimulus pulses, each the same as in Figure 3.10 but separated in time by a 1 ms interval between the end of the first pulse and the beginning of the second. Something that can generously be called an "integration" is visible in the membrane voltage response and in the Na$^+$ channel conductance. However, it is a nonlinear "integration" and is quite different from what would be obtained from a linear "leaky integrator" model of the membrane response. Moving the application of the second pulse closer to the end of the first pulse does not result in "better integrator" action; it results in an action potential.

In point of fact, axons do not make good "integrators." Their "hair trigger" response works against this form of signal processing. H-H-like models of *neurons*, on the other hand, often exhibit subthreshold responses that come much closer to the linear integrate-and-fire model so often used in neural *network* modeling. Even here, though, the integrator action is nonlinear, and

this reveals the approximate nature of the I&F model of the "mathematical neuron." The source of the nonlinearity is readily apparent from the conductance responses shown in the figures.

Exercises

Some of the following exercises require computation of the Hodgkin-Huxley model. You may either write your own computer program to implement Algorithm 3.1 or use and modify the MATLAB® version of this algorithm given in the appendix to this chapter.

1. It was shown in the text that the Katz concentrations for Na^+ and K^+ in squid implied the not unreasonable value of $V_r = -67.4$ mV for the resting potential of the membrane. According to the Nernst equation, what temperature is implicated for the E_{Na} and E_K this resting potential implies? Do you see any problems or contractions implied in this consequence? Describe and explain them.

2. Using Katz's numbers for Na^+ concentrations and Koester's and Siegelbaum's numbers for K^+ concentrations, find the Nernst potentials for Na^+ and K^+ at a temperature of 280 Kelvin. Then show that these potentials when combined with the Hodgkin-Huxley battery parameters implicate a resting potential in the range -62 ± 0.7 mV. What percentage uncertainty in the range of the experimental measurements does this imply? Is this a reasonable range?

3. Accepted data for squid places chloride concentrations at $[Cl^-]_o$ at 540 nM and $[Cl^-]_i$ in a range from 40 nM to 100 nM. At a temperature of 280 Kelvin, what is the range of Nernst potential implied by these figures? (Remember, the valence of chloride is -1). Using $V_r = -62$ mV, is chloride a reasonable hypothesis for explaining the Hodgkin-Huxley leakage potential?

4. The Hodgkin-Huxley Na^+ and K^+ currents for the membrane at rest are not compatible with the 3:2 ratio required by the Na^+-K^+ pump. Is it possible to modify the leakage circuit component of the Hodgkin-Huxley model to remove this discrepancy by assuming there are persistent Na^+, K^+ and possibly Cl^- channels already open at $V_r = -62$ mV? Use the Nernst potentials calculated at 280 Kelvin for the three ions (for chloride you have a range rather than one value). Remember that your modified leakage circuit must be equivalent to the Hodgkin-Huxley leakage circuit with its $G_{lk} = 0.3$ mS/cm^2 and its leakage potential of $10.613 - 62$ mV and the ratio of total Na^+ current to K^+ current must be 3:2.

5. The charge injected into a cell by a current source $I_s(t)$ is equal to the integral of the current from $t = 0$ to $t = \infty$. Show that a rectangular current pulse of amplitude I_{max} and width T_w injects the same amount of charge as an alpha-function pulse $I_{max} \cdot g^{(\alpha)}(t)$, where $g^{(\alpha)}(t)$ is given by (3.15), provided that the time constant of the alpha function equals $\exp(-1) \cdot T_w$.

6. Does the threshold for firing an action potential depend on the shape of the current pulse injected into the cell or does it only depend on the total charge injected? To find out, determine the threshold peak current I_{max} (within 0.2 µA/cm^2) for a rectangular pulse I_s of width $T_w = 5$ ms using a Hodgkin-Huxley simulation. Then repeat this for I_s given by an alpha function using the time constant determined in exercise 5. What do you conclude?

7. Using the Hodgkin-Huxley simulation, characterize the refractory period by determining the required I_{max} needed to stimulate a second action potential given that a first action potential was stimulated with the I_{max} for the rectangular pulse found in exercise 6. Characterize the threshold from 10 to 20 ms after the application of the first pulse and fit an exponential curve function to your data.

MATLAB Script for Hodgkin-Huxley Simulation

```
1  % file HHSquid.m Hodgkin-Huxley model using Euler's method
2  % This script allows up to two current pulses to be injected
3  % into the membrane to excite a response. The widths can
4  % be independently set, but the pulses cannot overlap. If pulse
5  % 2 is turned on before pulse 1 ends it replaces pulse 1.

6  clear; clf;
7  % maximal conductances (mS/cm^2); 1=K, 2=Na, 3=lk;
8  % membrane capacitance is 1 uF/cm^2
9   g(1)=36; g(2)=120; g(3)=0.3;

10 % battery voltage (mV) relative to resting potential; 1=K, 2=Na;
      3=lk
11  E(1)=-12; E(2)=115; E(3)=10.613;

12 % variable initialization I_ext is in microamps/cm^2
13  I_ext=0; V=-10; x=zeros(1,3); x(3)=1; t_rec=0;
14  t_final=50; % t_final sets the time span of the simulation

15 % applied pulses parameters; T1=on time for pulse 1, T2=on
      time    for pulse 2
16 % Tw1 is the width of pulse 1, Tw2 is the width of pulse 2.
      I_on1 is the
17 % amplitude of pulse 1 in microamps/square cm, I_on2 is the
      amplitude of
18 % pulse 2. All times are in milliseconds. If T2>t_final the
19 % second pulse is not applied.

20  I_on1=2.5; I_on2=2.5; T1=10; T2=70; Tw1=5; Tw2=5;

21 % time step for integration in milliseconds
22  dt=0.01;

23 % integration by Euler's method
24 % computations for t < 0 establish initial conditions at t = 0.
25  for t=-30:dt:t_final
26     if t==T1; I_ext=I_on1; end  %turns on external current at
      t=T1
27     if t==T1+Tw1; I_ext=0; end   %turns off external current
28     if t==T2; I_ext=I_on2; end   %turns on second pulse
29     if t==T2+Tw2; I_ext=0; end   %turns off second pulse

30     %alpha parameters in H-H model
31     alpha(1)=(10-V)/(100*(exp((10-V)/10)-1));
32     alpha(2)=(25-V)/(10*(exp((25-V)/10)-1));
33     alpha(3)=0.07*exp(-V/20);

34     %beta parameters in H-H model
35     beta(1)=0.125*exp(-V/80);
36     beta(2)=4*exp(-V/18);
37     beta(3)=1/(exp((30-V)/10)+1);

38     %time constants (msec) and asymptotic values
39     tau=1./(alpha+beta);
40     x_0=alpha.*tau;

41     %Euler integration
42     x=(1-dt./tau).*x+dt./tau.*x_0;

43     %conductance calculations
44     gnmh(1)=g(1)*x(1)^4;
45     gnmh(2)=g(2)*x(2)^3*x(3);
46     gnmh(3)=g(3);

47     %membrane voltage update
48     I=gnmh.*(V-E);
49     V=V+dt*(I_ext-sum(I));

50     %plotting records
51     if t>=0;
52       t_rec=t_rec+1;
53       x_plot(t_rec)=t;
54       y_plot(t_rec)=V;
55       G(t_rec,1)=gnmh(1); % GK
56       G(t_rec,2)=gnmh(2); % GNa
57     end
58   end
59 plot(x_plot,y_plot); xlabel('Time (ms)'); ylabel('Relative
      Membrane Voltage (mV)');
60 figure;
61 plot(x_plot,G); xlabel('Time (ms)'); ylabel('Conductance
      (mS/cm^2)');
```